Chemical Physics Letters xxx (xxxx) 138815

Contents lists available at ScienceDirect

Chemical Physics Letters

journal homepage: www.elsevier.com/locate/cplett

Research paper

Noncovalent interactions in catechol/ammonium-rich adhesive motifs: Reassessing the role of cation-π complexes?

Alessandro Ferretti [a], Giacomo Prampolini [a,*], Marco d'Ischia [b]

[a] Istituto di Chimica dei Composti OrganoMetallici (ICCOM-CNR), Area della Ricerca, via G. Moruzzi 1, I-56124 Pisa, Italy
[b] Dipartimento di Scienze Chimiche, Universitá di Napoli Federico II, I-80126 Napoli, Italy

ARTICLE INFO

Keywords:
Noncovalent interactions
Phenolic systems
Underwater adhesion
Catechol
Cation-pi

ABSTRACT

Cation-π interactions between ammonium and catechol groups provide a commonly held paradigm in the complex interplay of noncovalent forces that govern both biological phenomena, such as underwater adhesion in mussel byssus and other marine organisms, and aggregation processes in self-assembly of catecholamine-derived polymers. However, closer consideration of the peculiar properties of the catechol functionality, that features two adjacent phenoxyl groups endowed with chelating properties, would suggest operation of alternate interaction geometries besides typical cation-π. Following previous studies on various alkali metal cations, we report herein compelling computational evidence in favor of a so far overlooked σ-type interaction between the ammonium cation and the catechol system, as the most important contributor to binding, far exceeding the cation-π component. The present findings would hence prompt an experimental and theoretical reassessment of the actual importance of cation-π against σ-type interaction between ammonium and catechol groups in underwater adhesive patterns. In this framework, the catechol-ammonium interaction energy potential surfaces herein reported may provide an improved reference to approach more realistic natural and synthetic adhesion models encompassing other participating molecules/ions and the role of the solvent.

1. Introduction

The complex interplay among different types of noncovalent interactions (NCI) [1–3] plays a fundamental role in several biological processes and phenomena. In particular, the competition among hydrogen bonding [4], π-π [5] and cation-π [6] interactions dominates selective and tunable structure-dependent molecular recognition in inhibitor-enzyme, ligand-receptor, ligand-transporter, and hapten-antibody binding [7]. However, one of the most remarkable examples of biological phenomena that hinge on cation-π interactions is represented by underwater adhesion in marine mussels and other aquatic organisms [8–12]. Based on commonly accepted models, adhesion to the rock surface is mainly attributed to the exposed catechol residues of DOPA [13,14,8,15] in a fashion that is favored by the proximity of protonated amine groups in lysine residues [16], while other authors find that there is a synergy between lysine and DOPA in interfacial adhesion independently from their relative position [17,18]. The catechol moiety of DOPA can also establish surface dependent interaction processes [19] and the replacement of catechol with phenyl groups is usually associated with a worse performance [18]. Following the elucidation of catechol-ammonium interactions in mussel byssus, considerable attention has been devoted to the design of bioinspired adhesive materials like polydopamine for a broad range of technological and biomedical applications [10,12,20–23]. The importance of the medium conditions in under water adhesion has been emphasized in several instances. For example it has been reported that cationic-aromatic sequences can yield strong electrostatic adhesion of hydrogels in seawater, where high ionic strength environmental conditions operate [24]. The marked complexity of this phenomenon has been highlighted in recent reports demonstrating that amine-catechol pairs may have anti-synergetic effects suggesting an unexpectedly negative impact of this interaction in underwater adhesion [25].

Concomitant to, and in support of, progressing experimental approaches, growing interest has been devoted in the past decade to the setup and application of various computational methods suitable for the investigation of non-covalent interactions [26,3], including cation-π, [27] settled between van der Waals homo- or heterodimers *in vacuo*. As far as cation-π complexes are concerned, most of the attention was focused on the interaction between benzene and alkali metal cations [28–34], or small polyatomic ions such as NH_4^+ [35–38]. In line with

* Corresponding author.
E-mail address: giacomo.prampolini@pi.iccom.cnr.it (G. Prampolini).

https://doi.org/10.1016/j.cplett.2021.138815
Received 22 April 2021; Received in revised form 1 June 2021; Accepted 6 June 2021

the advent of the idea that cation-π interaction may be significant in biological processes, also phenol or catechol complexes with cations have been investigated to some extent [39–42], including polyatomic ones, such as ammonium and protonated amines [43,37,38]. In this framework, we have also very recently investigated [34,44] cation-aromatic non covalent dimers by means of the MP2^{mod} method [45,46], a very accurate, yet computationally convenient protocol for the calculation of the interaction energy (ΔE). Interestingly, notwithstanding the fact that the MP2^{mod} protocol was originally proposed and applied by our group for aromatic interactions, [45–52] its reliability in handling interaction between aromatic species and cations was very recently assessed with respect to very accurate ΔE reference data [34,44]. Thanks to such validation, the computational convenience of the MP2^{mod} protocol allowed us to confidently carry out a wide and deep exploration of the ΔE multidimensional surface [44], which highlighted effects that were probably overlooked in a more limited scan. A most noticeable outcome of this approach was the finding that installment of phenolic hydroxyl groups onto the benzene ring causes a gradual shift in phenolic systems from pure cation-π interactions (as in benzene) to strong and dominant σ-type cation-lone pair interactions engaging the OH groups in the plane of the aromatic ring [44]. Herein, we exploit the aforementioned MP2^{mod} features in handling both cation-π and σ-type interactions, to investigate the the complexes formed by ammonium ions and catechol. Furthermore, to better elucidate the role of the hydroxyl substituents, we also present the results obtained with the same ions interacting with phenol and benzene. On the one hand, aim of this computational study is to probe on a preliminary basis the potential of σ-type versus cation-π interactions in the catechol-ammonium binding mechanisms, with a view to setting the basis for a detailed reassessment of the mechanism in systems and processes of biological and technological relevance. On the other hand, the interaction energy surfaces here reported, reliably sampled at QM level for a large number of ion–molecule arrangements, can be promptly employed as reference to tune lower level models, e.g. classical FFs [50,53–55], which are fundamental to take into account other players as solvent, other ionic species and/or biological embedding.

2. Computational details

Unless otherwise stated, following the approach adopted in our previous work on cation–π interaction with alkali metal ions [34,44], the geometry of all considered monomers was initially optimized at B3-LYP/cc-PVTZ level, and kept frozen during the single-point calculations of the interaction energy ΔE. The latter were computed in the supermolecule approach, always applying the standard Counterpoise correction [56] to take care of the basis set superposition error. Reference CCSD(T) calculations, performed for validation purposes, were carried out with the 6-311 + G(2d,p) basis set.

All interaction energy curves, dimer optimizations and interaction energy landscapes were computed by means of the MP2^{mod} method, recently tuned and validated by us to handle cation–π [34] and σ-type [44] interactions. The excellent compromise between accuracy and computational cost granted by the MP2^{mod} approach exploits an error compensation between the well-known overestimation of the interaction strength, delivered by the Möller-Plesset Second Order Perturbation Theory (MP2) in estimating aromatic interactions [57], and the underestimation caused by the reduced basis set dimensions. Moreover, following the ideas of the early work of Kroon-Batenburg and Van Duijneveldt [58] and Hobza's group [59,60], the exponents of the polarization functions of the employed basis set are further optimized to reproduce reference CCSD(T) data. In the present work, following the approach proposed in Ref. [[34]], we employed specifically modified basis sets for the considered aromatic molecules, 6-31G(0.32,0.20) [34, 46] for benzene and 6-31G(0.27, 0.34, 0.36) [51,34] for phenol and catechol, whereas the standard 6-311 + G(2d,p) for the either NH_4^+ or $MeNH_3^+$. All calculations were carried out with the GAUSSIAN16 suite of programs [61].

3. Results

3.1. cation–π and σ-type interaction energy curves

The formation of a non covalent complex between an aromatic ring and the NH_4^+ ion can take place along two different directions, as displayed in Fig. 1. On the one hand, when the cation approaches the ring along the $\hat{C}_6$ axis of the aromatic carbon skeleton, $\mathbf{R}_\pi$, the stabilizing effect of the cation-π interaction is well known [6]. On the other hand, if the nitrogen atom lies within the plane containing the ring and is moved toward the ring along the line bisecting the C–C bond, $\mathbf{R}_\sigma$, the σ-type interaction between cation and the hydroxyl substituents is expected to be maximized [34,40,44]. Notwithstanding NH_4^+ can approach the aromatic species with different orientations (see Figs. S1 and S2 in the Supplementary Information), i.e. pointing one (**1H**), two (**2H**) or three (**3H**) hydrogen atoms toward the ring, only minor differences, amounting to at most 10% (see Figs. S3 - S8), were found among the possible NH_4^+ arrangements. Hence, for the sake of clarity, only the data for the geometries with NH_4^+ pointing two hydrogens in an eclipsed conformation (**2He**, see also Fig. 1) are displayed in Fig. 2, whereas a more detailed presentation of the results for each specific conformer can be found in the Supplementary Information.

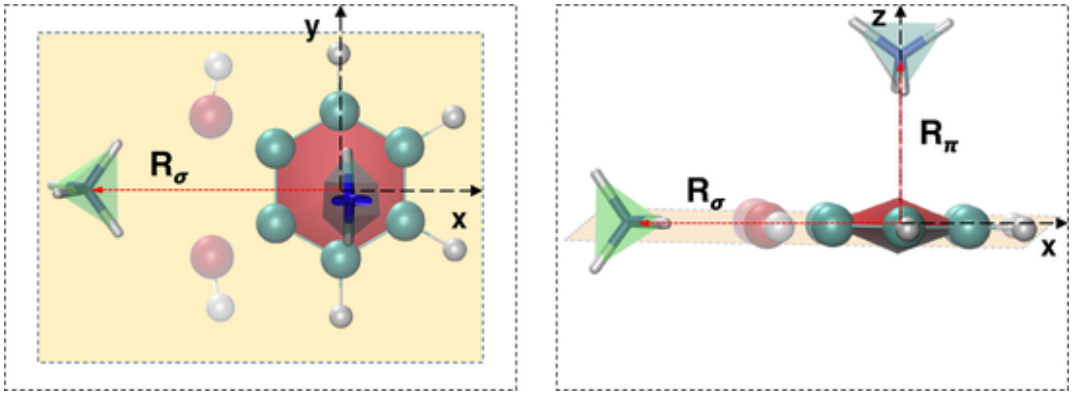

Fig. 1. Top (left) and side (right) views of the approaching R_π and R_σ directions for the considered cation-aromatic species pairs. The aromatic carbon skeleton, shared among benzene, phenol and catechol is evidenced in red, while the possible -OH substituents are shown with shaded colors. The NH_4^+ ion is highlighted in cyan or green when involved in cation–π or σ-type interactions, respectively.

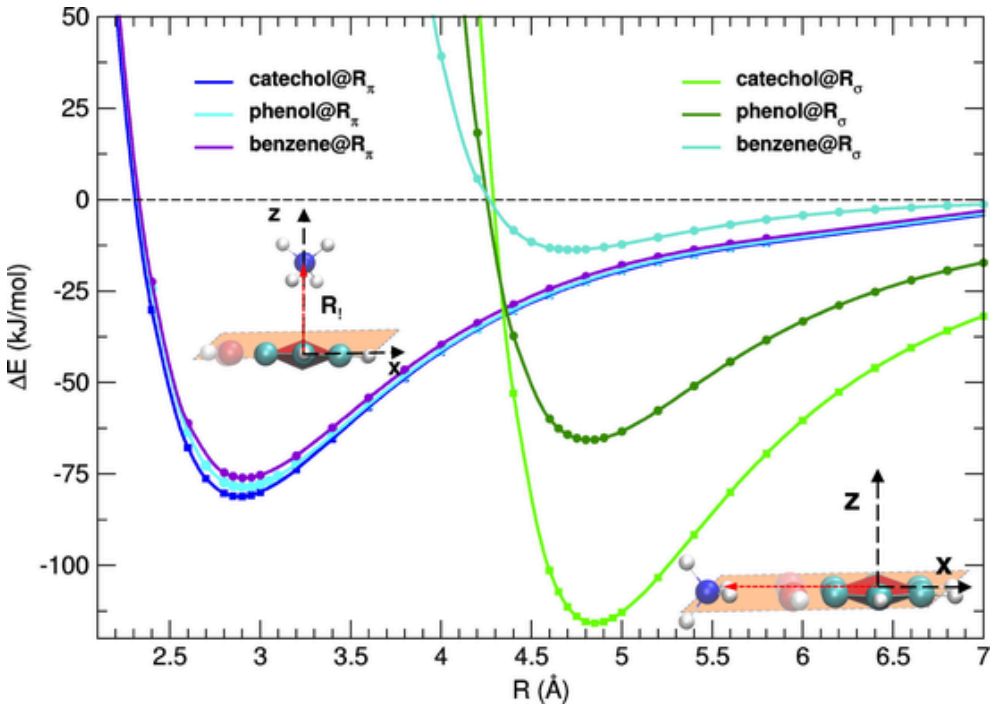

Fig. 2. Computed MP2^{mod} interaction energy (ΔE, kJ/mol) profiles of NH_4^+ complexes with catechol (blue and green lines), phenol (cyan and dark green) and benzene (violet and turquoise). The cation–π interactions, sketched in the left inset, are all displayed with bluish color, whereas σ-type ones (right inset) are highlighted with greenish tones.

Fig. 2 shows the interaction energy curves computed at MP2^{mod} level [34,44] for complexes formed by an aromatic molecule (either catechol, phenol or benzene) and the NH_4^+ ion, approaching either along the $\mathbf{R}_\pi$ or $\mathbf{R}_\sigma$ direction. As far as catechol is concerned, relatively strong cation–π interactions are established when the ion is shifted along the $\mathbf{R}_\pi$ direction (blue lines), i.e. "on top" of the π cloud. Both the interaction strength (~ 80 kJ/mol) and the minimum distance (~2.9 Å) are close to those recently reported by us for catechol-K^+ complexes (78 kJ/mol and 2.9 Å) [34,44]. As shown in Fig. S3 and Table A in the Supplementary Information, besides a slight preference of about 10 kJ/mol for the **2He** configuration, these cation–π driven conformations are stable regardless the orientation of the N-H axes with respect to the aromatic core, thus behaving similarly to a monoatomic ion. More interestingly, an even stronger interaction (~110 kJ/mol) clearly appears also along the $\mathbf{R}_\sigma$ direction (green lines), when the NH_4^+ ion approaches the hydroxyl groups, but is less close to the aromatic π cloud. It should be noted here that such very favorable σ-type interaction energy largely counterbalances the internal energy loss in catechol, due to the 180◦ torsion of the O–H bond and the consequent breaking of the intramolecular H-bond, which takes place to allow the cation to settle closer to the oxygen atoms, as previously found for alkali metal cations [34,44]. It might be also worth mentioning that, at difference with the cation–π interactions, the **2He** conformer, where two NH_4^+ hydrogens closely interact with the neighboring catechol oxygen atoms, is more stable (~15 kJ/mol, see Table B in the Supplementary Information) than the **2Hs** staggered one. These findings confirm that the alternative, yet very stable, in-plane σ-type conformation, recently reported for catechol complexes with alkali metal ions [34,44], can play a crucial role also in the chemistry of the catechol moiety with the NH_4^+ ion. Additionally, the direct interaction of the cation with the oxygens lone pair, characterizing the σ-type-dimers [40,44] with alkali metals, is in the present case also enforced by the favorable forces that can be established between the oxygen lone pair and the ammonium hydrogens, as suggested by the difference between the **2He** and **2Hs** conformers.

3.2. *Effect of phenoxyl substitution on σ-type interaction energy curves*

To further investigate the factors underlying the unusual strength of the σ-type interaction, we have computed the same ΔE profiles for the phenol-NH_4^+ and benzene-NH_4^+ pairs. The curves are displayed in Fig. 2, while the resulting minima are reported in Table 1. The comparison among the three aromatic moieties yields indeed a clear rationale of the relationship between σ-type interaction's strength and the presence of the hydroxyl substituents. As far as the cation–π interactions are concerned, in agreement with the results obtained for alkali metal cations [34], both the position and the depth of the minimum are almost unchanged in going from catechol to benzene and the difference in the ΔE profiles are negligible. The reliability of such results, obtained at MP2^{mod} level, was validated through the comparison with highly accurate Coupled Cluster (CC) calculations, purposely carried out with Single, Double, and perturbatively included connected Triple excitations (CCSD(T)) for few selected conformations of the benzene-NH_4^+ complexes (see Table E for details): the final standard deviation with respect to CCSD(T), of ~5 kJ/mol, is in excellent agreement with the results recently obtained for alkali metals [34,44], thus allowing us to confi-

Table 1
Minimum interaction energies (ΔE_0) and noncovalent equilibrium bond lengths ($\mathbf{R}_\pi^0$ and $\mathbf{R}_\sigma^0$) computed at MP2^{mod} level for benzene-NH_4^+, phenol-NH_4^+ and catechol-NH_4^+ dimers along the $\mathbf{R}_\pi$ and $\mathbf{R}_\sigma$ directions displayed in Fig. 1. The labels **2He** and **2Hs** refer to the orientation of the N-H bonds with respect to the aromatic moiety, as shown in detail in Figures S1 and S2 in the Supplementary Information.

Molecule	cation–π			σ-type		
	Label	$\mathbf{R}_\pi$ (Å)	ΔE_0 (kJ/mol)	Label	$\mathbf{R}_\sigma$ (Å)	ΔE_0 (kJ/mol)
catechol	**2He**	2.90	−81.2	**2He**	4.85	−115.8
phenol	**2Hs**	2.90	−80.0	**2He**	4.80	−65.7
benzene	**2He**	2.90	−76.1	**2Hs**	4.50	−18.2

dently apply the MP2^{mod} method to further investigate NH_4^+ complexes with aromatic moieties.

Turning to the the σ-type-interactions established along the $\mathbf{R}_\sigma$ direction, striking differences instead appear when one or two phenolic hydroxyl groups of catechol are replaced with an aromatic hydrogen. In phenol-NH_4^+ complexes (dark green lines in Fig. 2) the depth of the σ-type minimum is around 15 kJ/mol smaller than the one found for the same pair along $\mathbf{R}_\pi$, and ~50 kJ/mol less stable than its catechol-NH_4^+ counterpart. Furthermore, as evidenced in Fig. S6 and Table D in the Supplementary Information, the **2He** conformer is still the most stable, but the differences with the other arrangements are remarkably reduced. On the same foot, the removal of the second -OH substituent definitively contributes to undermine σ-type stability in favor of cation–π one. In benzene, the σ-type's interaction strength (turquoise lines) is further reduced to less than 20 kJ/mol, with the most stable NH_4^+ configuration being **2Hs**, where the repulsion between the NH_4^+'s hydrogens and the aromatic ones is smaller (see Fig. S8 and Table F for details).

3.3. cation–π and σ-type interaction energy landscapes

The enhanced stability of σ-type conformers in catechol versus other aromatic systems may be taken as evidence for a peculiar behavior of the o-dihydroxy functionality, e.g. in DOPA, versus other aromatic systems lacking phenoxyl groups in the o-substitution pattern, e.g. tyrosine and phenylalanine. Nonetheless, before hypothesizing a major role of σ-type interactions, possibly detrimental to the settlement of competing cation–π ones, it is necessary to rule out both the existence of other "hybrid" minima and the presence of inter-conversion channels, through which the cation could easily migrate from one configuration to the other. To this end, exploiting MP2^{mod} computational convenience, we sampled the whole [$\mathbf{R}_\pi$, $\mathbf{R}_\sigma$] configurational space see Fig. 3.b for definition), through the calculation of around one thousand *ab initio* catechol-NH_4^+ interaction energies. Fig. 3.a shows the resulting interaction energy landscape $\Delta E(\mathbf{R}_\sigma, \mathbf{R}_\pi)$. The σ-type minimum region is clearly visible on the right, and it covers a rather broad range both in $\mathbf{R}_\sigma$ (3.5–5.5 Å) and in $\mathbf{R}_\pi$ (-3.0–3.0 Å). Conversely, the two degenerate cation–π minima (localized at $\mathbf{R}_\pi 3\simeq \pm$ Å) are less evident, since the wells are smoothly extended along $\mathbf{R}_\sigma$, in particular toward positive $\mathbf{R}_\sigma$, i.e. closer to the σ-type minimum region. Both minima were better characterized through a geometry optimization, again carried out at MP2^{mod} level, starting from either the cation–π or the σ-type region. The resulting minima, displayed respectively in Fig. 3.c and d, can still be classified as cation–π and σ-type, since in the former NH_4^+ is centered on top of the aromatic π cloud, along the axis perpendicular to the ring, whereas in the latter it is close the the hydroxyl groups, with its hydrogens pointing toward the catechol's oxygen atoms, though with the N atom slightly out of the plane containing the ring. The significantly larger stability of the σ-type configuration is again confirmed by computing the interaction energy at the two optimized geometries, reported in Table 2. To exclude possible inaccuracies of the MP2^{mod} predictions, this result has been further validated at CCSD(T) level, by computing again the interaction energy of the two conformers with the higher level method: despite a systematic MP2^{mod} overestimation, slightly larger than the one previously found for the complexes involving benzene, both methods agree in indicating the σ-type arrangement as the most stable and, more important, in the assessment of the ratio between the two investigated geometries (~1.5).

To further explore and characterize the possible paths interconnecting the two binding points, additional interaction energy profiles were computed at MP2^{mod} level again scanning the $\mathbf{R}_\sigma$ coordinate, but increasing the number of sampled $\mathbf{R}_\pi$ heights. The results are shown in Fig. 4, where the catechol-NH_4^+ configurations corresponding to the resulting minima and barriers are displayed in the insets. At short $\mathbf{R}_\pi$ distances, a significant barrier separates two minima: a first one, solely ascribable to cation-π interactions, where the ion center of mass is located along the ring normal axis ($\mathbf{R}_\sigma$ ~0 Å), and a second, more stable one, where the NH_4^+ cation is shifted toward the oxygen atoms lone-pairs ($\mathbf{R}_\sigma$ ~3.5 Å). The interaction energy difference between the two minima, as well as the barriers height, sensibly decreases as the ion steps away from the π cloud. At $\mathbf{R}_\pi > 2.8$ Å, the two minima are almost degenerate, and the barrier separating them is reduced by almost an order of magnitude. Despite these results suggest that at room temperature an

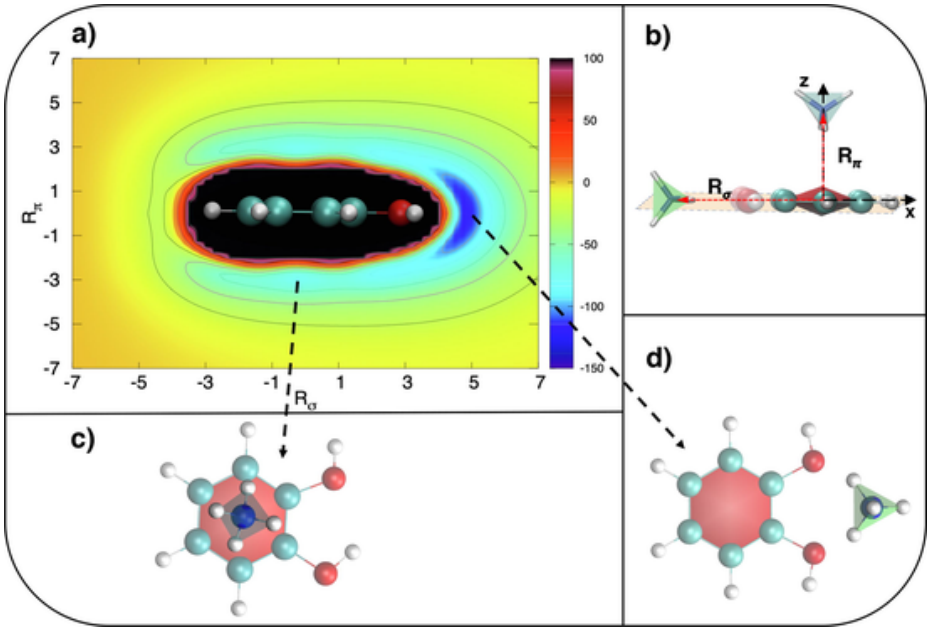

Fig. 3. a) Two dimensional plot of the interaction energy (ΔE, kJ/mol, in the color palette) of the catechol-NH_4^+ pair along the $\mathbf{R}_\sigma$ and $\mathbf{R}_\pi$ coordinates; b) Reference system. cation–π and σ-type arrangements of the NH_4^+ cation are highlighted in blue and green, respectively; c) Optimized geometry for catechol-NH_4^+ dimer in the cation–π conformation; d) Optimized geometry of the catechol-NH_4^+ dimer in the σ-type conformation.

Table 2
Interaction energies computed at MP2^{mod} and CCSD(T) level, at the cation–π (ΔE^{π}) and σ-type (ΔE^{σ}) geometries, optimized at MP2^{mod} level. The ratio $R_{\sigma/\pi}$, between the σ-type and cation–π ΔEs, is reported in the third row for both methods. On the same foot, the employed CPU time is shown in the last row.

	MP2^{mod}	CCSD(T)
ΔE^{π} (kJ/mol)	−93.2	−80.0
ΔE^{σ} (kJ/mol)	−142.2	−132.0
$R_{\sigma/\pi}$	1.4	1.6
CPU time (min)	9	18300 (>12 days)

NH_4^+ ion approaching the catechol molecule will preferentially visits σ-type-arrangements, a complex interplay among different configurations should be expected, with catechol-NH_4^+ pairs stabilized through a balance of "pure" cation–π to more hybrid σ-type interactions.

3.4. *Catechol*–$MeNH_3^+$ *complexes*

The results so far discussed indicate that phenol and catechol may interact with the NH_4^+ ion via markedly different mechanisms, and highlight the decisive role of hydroxyl substituents in governing the position of the cation with respect to the aromatic cloud and, consequently, the stability of the resulting complexes. It is thus of interest to ascertain whether and to what extent the present results hold for larger NH_4^+ functionalized cations, as in biologically relevant molecules. Accordingly, the present investigation was extended from the simple NH_4^+ cation to a protonated primary amine, the methyl ammonium ($MeNH_3^+$), computing again the interaction energy profiles at MP2^{mod} level for the cation–π and σ-type configurations of its complexes with both phenol and catechol. Fig. 5 shows the comparison of the computed energy profiles for catechol and phenol complexes with both $MeNH_3^+$ and NH_4^+ ions.

Since negligible differences were found (see Fig. S10 in the Supplementary Information) in the trends of the interaction energy with respect to the ion orientation, we have here limited the comparison to the most stable conformations, i.e. the **2He** ones. The minimum ΔE and the noncovalent bond length for catechol and phenol complexes with either the NH_4^+ or $MeNH_3^+$ ion are summarized in Table 3. For both aromatic species, the presence of the methyl induces in all cases a decrease in the well depth, more evident for σ-type interactions than for cation–π: the difference in ΔE_{π} with respect to the simple NH_4^+ ion (~4% for both catechol and phenol) is about half the one found in ΔE_{σ} (~8% for phenol and ~10% for catechol). Nonetheless, the main result observed for the NH_4^+ ion appears to hold also when considering a primary amine: while in phenol-cation complexes the cation–π "on top" interaction is stronger than the "in plane" σ-type one, in catechol-cation aggregates the picture is reversed, and the σ-type arrangements are almost twice more stable than the more investigated cation–π ones.

4. Conclusions

Computational evidence is presented, suggesting that so far overlooked in-plane σ-type interactions at the o-diphenol functionality may play a crucial and hitherto unrecognized role in the binding of ammonium cations to catechol π-systems. These results would point to an integrated and more complex scenario in which a three-dimensional network of non-covalent orthogonal interactions would provide a robust and synergic framework of cooperative effects imparting exceptional strength to byssus proteins. Further evidence in support of these conclusions is required to delineate a more realistic model for the interplay of non-covalent catechol-ammonium interactions in, e.g., mussel byssus and polydopamine and to orient further advances in the rational design of advanced underwater adhesives. From a computational point of view, the present results could serve as reference to validate or refine the classical force-field based simulations, which are often built upon rough and incomplete descriptions, and to assess their suitability to account for both cation-π and σ-type interactions toward more realistic models of underwater adhesion. An important issue that needs to be addressed in future computational efforts concerns the role of the counterion, since the latter can likely affect the conformation of the OH bonds. The need to extend the investigation to ternary aromatic-cation–anion systems has emerged in recent studies indicating that aromatic groups can enhance the electrostatic interactions of cationic residues to negatively charged surfaces within co-polymeric scaffolds even in a high

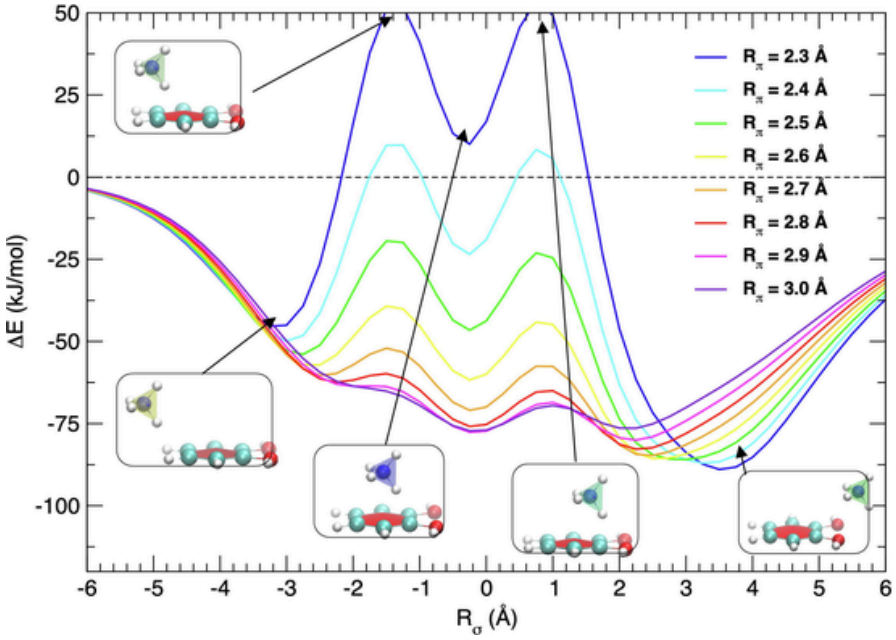

Fig. 4. $\mathbf{R}_{\sigma}$ interaction energy profiles computed at MP2^{mod} level for catechol-NH_4^+ complexes at fixed $\mathbf{R}_{\sigma}$ heights. In the insets, The dimer configurations (at $\mathbf{R}_{\sigma}$ = 2.3 Å) corresponding to the local minima and to the barriers are shown ion the insets.

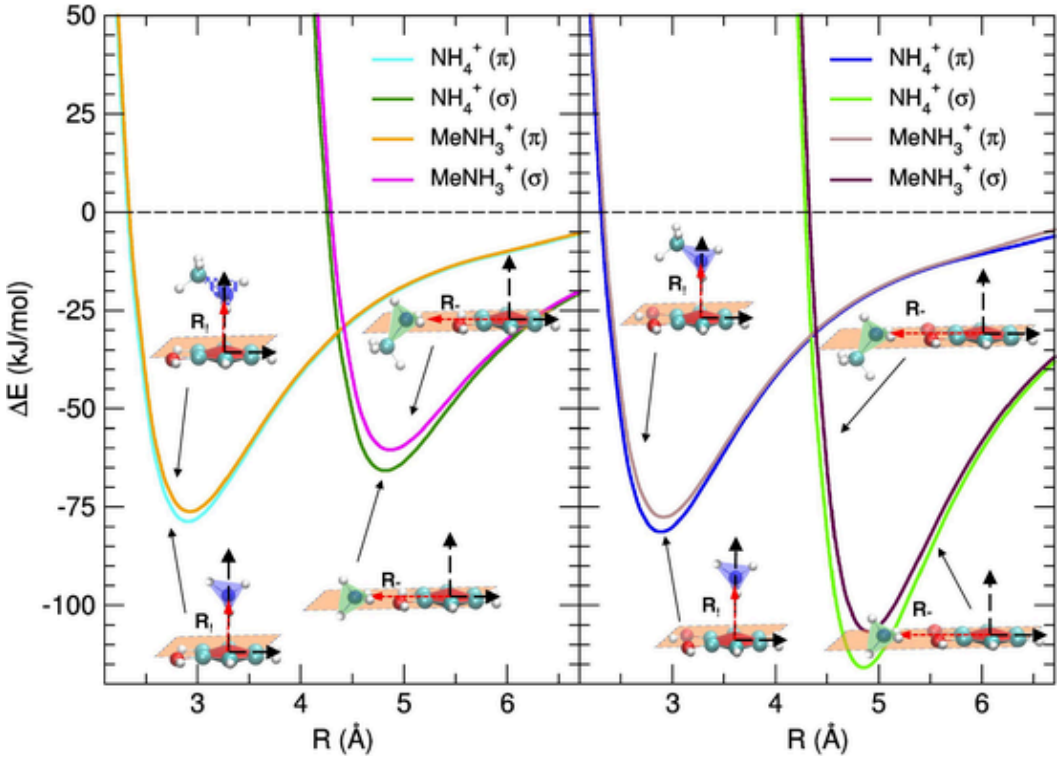

Fig. 5. Computed MP2*mod* interaction energy (ΔE, kJ/mol) profiles of NH_4^+ and $MeNH_3^+$ complexes with phenol (left panel) and catechol (right panel). The cation–π and σ-type arrangements are sketched for reference in the insets, and evidenced in blue and green, respectively.

Table 3
Minimum interaction energies ($\Delta E_\pi, \Delta E_\sigma$) and noncovalent equilibrium bond lengths ($\mathbf{R}_\pi^0$ and $\mathbf{R}_\sigma^0$) computed at MP2*mod* level for catechol–NH_4^+ and catechol–$MeNH_3^+$ complexes along the $\mathbf{R}_\pi$ and $\mathbf{R}_\sigma$ directions displayed in Fig. 1.

Complex	cation–π		σ-type	
	$\mathbf{R}_\pi$ (Å)	ΔE_π (kJ/mol)	$\mathbf{R}_\sigma$ (Å)	ΔE_σ (kJ/mol)
catechol–NH_4^+	2.90	−81.2	4.85	−115.8
catechol–Me-NH_3^+	2.90	−77.6	4.90	−106.6
phenol–NH_4^+	2.90	−78.8	4.80	−65.7
phenol–Me-NH_3^+	2.90	−76.1	4.85	−60.4

ionic-strength medium. It is thus argued that proximal aromatic systems can preserve the integrity of cation–anion binding even under high ionic strength conditions where screening effects may usually operate.

CRediT authorship contribution statement

Alessandro Ferretti: Conceptualization, Investigation, Writing - original draft. **Giacomo Prampolini:** Conceptualization, Methodology, Data curation, Writing - review & editing, Visualization. **Marco d'Ischia:** Conceptualization, Writing - review & editing.

Declaration of Competing Interest

The authors declare that they have no known competing financial interests or personal relationships that could have appeared to influence the work reported in this paper.

Acknowledgements

M.d.I. kindly acknowledges Italian Ministry of Research (MIUR) for financial support (PRIN, Grant No.: 2017YJMPZN).

Appendix A. Supplementary material

Supplementary data associated with this article can be found, in the online version, at https://doi.org/10.1016/j.cplett.2021.138815.

References

[1] A. Stone, The Theory of Intermolecular Forces, Oxford University Press, 2013.
[2] S. Scheiner, Noncovalent Forces, Springer International Publishing, Switzerland, 2015.
[3] P. Hobza, J. Rezáč, Introduction: Noncovalent Interactions, Chem. Rev. 116 (2016) 4911–4912.
[4] G.R. Desiraju, A Bond by Any Other Name Angew, Chem. Int. Ed. 50 (2011) 52–59.
[5] D. Fagnani, A. Sotuyo, Castellano R, Comprehensive Supramolecular Chemistry II, Elsevier, 2017, pp. 121–148.
[6] J.C. Ma, D.A. Dougherty, The cation-π interaction, Chem. Rev. 97 (1997) 1303–1324.
[7] Z. Liang, Q.X. Li, π–Cation Interactions in Molecular Recognition: Perspectives on Pharmaceuticals and Pesticides, J. Agric. Food Chem. 66 (2018) 3315–3323.
[8] J.H. Waite, Mussel adhesion - Essential footwork, J. Exp. Biol. 220 (2017) 517–530.
[9] H. Birkedal, Mimicking mussel mechanics, Nat. Chem. 9 (2017) 408–409.
[10] P. Kord Forooshani, B.P. Lee, Recent approaches in designing bioadhesive materials inspired by mussel adhesive protein, J. Pol. Sci. A 55 (2017) 9–33.
[11] A.H. Hofman, I.A. van Hees, J. Yang, M. Kamperman, Bioinspired Underwater Adhesives by Using the Supramolecular Toolbox, Adv. Mater. 30 (2018).
[12] A. Andersen, Y. Chen, H. Birkedal, Bioinspired metal-polyphenol materials: Self-healing and beyond Biomimetics. 4 (2019).
[13] W. Wei, J. Yu, C. Broomell, J.N. Israelachvili, J.H. Waite, Hydrophobic enhancement of dopa-mediated adhesion in a mussel foot protein, J. Am. Chem. Soc. 135 (2013) 377–383.
[14] M.V. Rapp, G.P. Maier, H.A. Dobbs, N.J. Higdon, J.H. Waite, A. Butler, J.N. Israelachvili, Defining the Catechol-Cation Synergy for Enhanced Wet Adhesion to Mineral Surfaces, J. Am. Chem. Soc. 138 (2016) 9013–9016.
[15] T. Priemel, R. Palia, M. Babych, C.J. Thibodeaux, S. Bourgault, M.J. Harrington, Compartmentalized processing of catechols during mussel byssus fabrication determines the destiny of DOPA Proc, Natl. Acad. Sci. USA 117 (2020) 7613–7621.
[16] M. Shin, J.Y. Shin, K. Kim, B. Yang, J.W. Han, N.K. Kim, H.J. Cha, The position of lysine controls the catechol-mediated surface adhesion and cohesion in underwater mussel adhesion, J. Colloid Interface Sci. 563 (2020) 168–176.
[17] G.D. Degen, P.R. Stow, R.B. Lewis, R.C. Andresen Eguiluz, E. Valois, K. Kristiansen, A. Butler, J.N. Israelachvili, Impact of Molecular Architecture and Adsorption Density on Adhesion of Mussel-Inspired Surface Primers with Catechol-Cation Synergy, J. Am. Chem. Soc. 41 (2019) 18673–18681.

[18] B.D.B. Tiu, P. Delparastan, M.R. Ney, M. Gerst, P.B. Messersmith, Cooperativity of Catechols and Amines in High-Performance Dry/Wet Adhesives Angew, Chemie - Int. Ed. 59 (2020) 16616–16624.

[19] T. Utzig, P. Stock, M. Valtiner, Resolving Non-Specific and Specific Adhesive Interactions of Catechols at Solid/Liquid Interfaces at the Molecular Scale Angew, Chem. Int. Ed. 55 (2016) 9524–9528.

[20] M.A. Gebbie, W. Wei, A.M. Schrader, T.R. Cristiani, H.A. Dobbs, M. Idso, B.F. Chmelka, J. Herbert Waite, J.N. Israelachvili, Tuning underwater adhesion with cation-πinteractions, Nat. Chem. 9 (2017) 473–479.

[21] S. Kim, H. Young Yoo, J. Huang, Y. Lee, S. Park, Y. Park, S. Jin, Y. Mee Jung, H. Zeng, D. Soo Hwang, Y. Jho, Salt Triggers the Simple Coacervation of an Underwater Adhesive When Cations Meet Aromatic πElectrons in Seawater, ACS Nano 11 (2017) 6764–6772.

[22] S. Park, S. Kim, Y. Jho, D.S. Hwang, Cation–π Interactions and Their Contribution to Mussel Underwater Adhesion Studied Using a Surface Forces Apparatus: A Mini-Review, Langmuir 35 (2019) 16002–16012.

[23] Y. Li, Y. Cao, The molecular mechanisms underlying mussel adhesion, Nanoscale Adv. 1 (2019) 4246–4257.

[24] L. Xie, L. Gong, J. Zhang, L. Han, L. Xiang, J. Chen, J. Liu, B. Yan, H. Zeng, A wet adhesion strategy via synergistic cation-$\pi$and hydrogen bonding interactions of antifouling zwitterions and mussel-inspired binding moieties, J. Mater. Chem. A 7 (2019) 21944–21952.

[25] M. Shin, Y. Park, S. Jin, Y.M. Jung, H.J. Cha, Two Faces of Amine-Catechol Pair Synergy in Underwater Cation-π Interactions, Chem. Mater. 33 (2021) 3196–3206.

[26] J. Rezáč, P. Hobza, Benchmark Calculations of Interaction Energies in Noncovalent Complexes and Their Applications, Chem. Rev. 116 (2016) 5038–5071.

[27] M.T. Rodgers, P.B. Armentrout, Cationic Noncovalent Interactions: Energetics and Periodic Trends Chem, Rev. 116 (2016) 5642–5687.

[28] J.C. Amicangelo, P.B. Armentrout, Absolute binding energies of alkali–metal cation complexes with benzene determined by threshold collision-induced dissociation experiments and ab initio theory, J. Phys. Chem. A 104 (2000) 11420–11432.

[29] D. Feller, A complete basis set estimate of cation–π bond strengths: Na^+(ethylene) and Na^+(benzene), Chem. Phys. Lett. 322 (2000) 543–548.

[30] J.P. Gallivan, D.A. Dougherty, A computational study of cation-π interactions vs salt bridges in aqueous media: Implications for protein engineering, J. Am. Chem. Soc. 122 (2000) 870–874.

[31] M.S. Marshall, R.P. Steele, K.S. Thanthiriwatte, C.D. Sherrill, Potential energy curves for cation-π interactions: Off-axis configurations are also attractive, J. Phys. Chem. A 113 (2009) 13628–13632.

[32] K. Ansorg, M. Tafipolsky, B. Engels, Cation–π Interactions: Accurate Intermolecular Potential from Symmetry-Adapted Perturbation Theory, J. Phys. Chem. B 117 (2013) 10093–10102.

[33] Y. Zhang, S. Chen, F. Ying, P. Su, W. Wu, Valence Bond Based Energy Decomposition Analysis Scheme and Its Application to Cation–π Interactions, J. Phys. Chem. A 122 (2018) 5886–5894.

[34] A. Ferretti, M. D'Ischia, G. Prampolini, Benchmarking Cation–π Interactions: Assessment of Density Functional Theory and Möller-Plesset Second-Order Perturbation Theory Calculations with Optimized Basis Sets ($mp2^{mod}$) for Complexes of Benzene, Phenol, and Catechol, J. Phys. Chem. A 124 (2020) 3445–3459.

[35] A.S. Mahadevi, G.N. Sastry, Cation-π interaction: Its role and relevance in chemistry, biology, and material science, Chem. Rev. 113 (2013) 2100–2138.

[36] A. Subha Mahadevi, G. Narahari Sastry, Cooperativity in Noncovalent Interactions, Chem. Rev. 116 (2016) 2775–2825.

[37] E.A. Orabi, G. Lamoureux, Cation-π Interactions between Quaternary Ammonium Ions and Amino Acid Aromatic Groups in Aqueous Solution, J. Phys. Chem. B 122 (2018) 2251–2260.

[38] E.A. Orabi, R.L. Davis, G. Lamoureux, Drude polarizable force field for cation–π interactions of alkali and quaternary ammonium ions with aromatic amino acid side chains, J. Comp. Chem. 41 (2020) 472–481.

[39] R. Amunugama, M.T. Rodgers, The Influence of Substituents on Cation-πInteractions. 4. Absolute Binding Energies of Alkali Metal Cation-Phenol Complexes Determined by Threshold Collision-Induced Dissociation and Theoretical Studies, J. Phys. Chem. A 106 (2002) 9718–9728.

[40] T.D. Vaden, J.M. Lisy, Characterization of hydrated Na + (phenol) and K + (phenol) complexes using infrared spectroscopy, J. Chem. Phys. 120 (2004) 721–730.

[41] T.D. Vaden, J.M. Lisy, Competition between cation-π interactions and intermolecular hydrogen bonds in alkali metal ion-phenol clusters, I. Phenol dimer J. Chem. Phys. 123 (2005) 74302.

[42] C. Kozmutza, F. Bartha, L. Udvardi, I. Varga, Study of the effect of metal ions on hydroxyl–containing molecules, Int. J. Quantum Chem. 107 (2007) 2730–2740.

[43] R. Sa, W. Zhu, J. Shen, Z. Gong, J. Cheng, K. Chen, H. Jiang, How Does Ammonium Dynamically Interact with Benzene in Aqueous Media? A First Principle Study Using the Car-Parrinello Molecular Dynamics Method, J. Phys. Chem. B 110 (2006) 5094–5098.

[44] G. Prampolini, M. d'Ischia, A. Ferretti, The Phenoxyl Group-Modulated Interplay of Cation-π and σ-type Interactions in the Alkaline Metal Series, Phys. Chem. Chem. Phys. (2020), https://doi.org/10.1039/D0CP03707A.

[45] V. Barone, I. Cacelli, O. Crescenzi, M. D'Ischia, A. Ferretti, G. Prampolini, G. Villani, Unraveling the interplay of different contributions to the stability of the quinhydrone dimer, RSC Adv. 4 (2014) 876–885.

[46] M. Jacobs, L. Greff Da Silveira, G. Prampolini, P.R. Livotto, I. Cacelli, Interaction Energy Landscapes of Aromatic Heterocycles through a Reliable yet Affordable Computational Approach, J. Chem. Theory Comput. 14 (2018) 543–556.

[47] C. Amovilli, I. Cacelli, S. Campanile, G. Prampolini, Calculation of the Intermolecular Energy of Large Molecules by a Fragmentation Scheme: Application to the 4-n-Pentyl-4′- Cyanobiphenyl (5CB) Dimer, J. Chem. Phys. 117 (2002) 3003.

[48] I. Cacelli, C.F. Lami, G. Prampolini, Force-field Modeling through Quantum Mechanical Calculations: Molecular Dynamics Simulations of a Nematogenic Molecule in its Condensed Phases, J. Comp. Chem. 30 (2009) 366–378.

[49] I. Cacelli, A. Cimoli, P.R. Livotto, G. Prampolini, An Automated Approach for the Parameterization of Accurate Intermolecular Force-Fields: Pyridine as a Case Study, J. Comp. Chem. 33 (2012) 1055.

[50] G. Prampolini, I. Cacelli, A. Ferretti, Intermolecular interactions in eumelanins: a computational bottom-up approach. I. small building blocks, RSC Adv. 5 (2015) 38513–38526.

[51] V. Barone, I. Cacelli, A. Ferretti, G. Prampolini, Noncovalent Interactions in the Catechol Dimer Biomimetics. 2 (2017) 18.

[52] I. Cacelli, F. Lipparini, L.G. da Silveira, M. Jacobs, P.R. Livotto, G. Prampolini, Accurate interaction energies by spin component scaled Moller-Plesset second order perturbation theory calculations with optimized basis sets (SCS-MP2(mod)): Development and application to aromatic heterocycles, J. Chem. Phys. 150 (2019) 234113.

[53] L. Greff da Silveira, M. Jacobs, G. Prampolini, P.R. Livotto, I. Cacelli, Development and Validation of Quantum Mechanically Derived Force-Fields: Thermodynamic, Structural, and Vibrational Properties of Aromatic Heterocycles, J. Chem. Theory Comput. 14 (2018) 4884–4900.

[54] A. Turupcu J. Tirado-Rives W.L. Jorgensen Explicit Representation of Cation-π Interactions in Force Fields with $\frac{1}{r^4}$ Nonbonded Terms J. Chem. Theory Comput. 16 2020 7184 7194

[55] M. Campetella, N. De Mitri, G. Prampolini, Automated parameterization of quantum-mechanically derived force-fields including explicit sigma holes: A pathway to energetic and structural features of halogen bonds in gas and condensed phase, J. Chem. Phys. 153 (2020) 44106.

[56] S. Boys, F. Bernardi, The Calculation of Small Molecular Interactions by the Differences of Separate Total Energies. Some Procedures with Reduced Errors, Mol. Phys. 19 (1970) 553–566.

[57] K.E. Riley, J.A. Platts, J. Řezáč, P. Hobza, J.G. Hill, Assessment of the Performance of MP2 and MP2 Variants for the Treatment of Noncovalent Interactions, J. Phys. Chem. A 116 (2012) 4159–4169.

[58] L. Kroon-Batenburg, F. Van Duijneveldt, The Use of a Moment-Optimized DZP Basis Set for Describing the Interaction in the Water Dimer, J. Mol. Struct. THEOCHEM 22 (1985) 185–199.

[59] J. Šponer, J. Leszczynski, P. Hobza, Nature of Nucleic Acid-Base Stacking: Nonempirical ab Initio and Empirical Potential Characterization of 10 Stacked Base Dimers. Comparison of Stacked and H-Bonded Base Pairs, J. Phys. Chem. 100 (1996) 5590–5596.

[60] J. Šponer, J. Leszczynski, P. Hobza, Base Stacking in Cytosine Dimer. A Comparison of Correlated Ab Initio Calculations with Three Empirical Potential Models and Density Functional Theory Calculations, J. Comput. Chem. 17 (1996) 841–850.

[61] M.J. Frisch, G.W. Trucks, H.B. Schlegel, G.E. Scuseria, M.A. Robb, J.R. Cheeseman, G. Scalmani, V. Barone, G.A. Petersson, H. Nakatsuji, X. Li, M. Caricato, A.V. Marenich, J. Bloino, B.G. Janesko, R. Gomperts, B. Mennucci, H.P. Hratchian, J.V. Ortiz, A.F. Izmaylov, J.L. Sonnenberg, D. Williams-Young, F. Ding, F. Lipparini, F. Egidi, J. Goings, B. Peng, A. Petrone, T. Henderson, D. Ranasinghe, V.G. Zakrzewski, J. Gao, N. Rega, G. Zheng, W. Liang, M. Hada, M. Ehara, K. Toyota, R. Fukuda, J. Hasegawa, M. Ishida, T. Nakajima, Y. Honda, O. Kitao, H. Nakai, T. Vreven, K. Throssell, J.A. Montgomery, Jr., J.E. Peralta, F. Ogliaro, M.J. Bearpark, J.J. Heyd, E. N. Brothers, K.N. Kudin, V.N. Staroverov, T.A. Keith, R. Kobayashi, J. Normand, K. Raghavachari, A.P. Rendell, J.C. Burant, S.S. Iyengar, J. Tomasi, M. Cossi, J.M. Millam, M. Klene, C. Adamo, R. Cammi, J.W. Ochterski, R.L. Martin, K. Morokuma, O. Farkas, J.B. Foresman, D.J. Fox, Gaussian16 Revision C.01; 2016; Gaussian Inc., Wallingford CT.